Eur. Phys. J. B **31**, 217–228 (2003)
DOI: 10.1140/epjb/e2003-00026-6

THE EUROPEAN PHYSICAL JOURNAL B

Light scattering by longitudinal acoustic modes in molecular supercooled liquids I: phenomenological approach

R.M. Pick[1], T. Franosch[2,a], A. Latz[3], and C. Dreyfus[4]

[1] UFR 925, UPMC, Paris, France
[2] Hahn-Meitner Institut, Glienicker Strasse 100, 14109 Berlin, Germany
[3] Technische Universität Chemnitz, 09107 Chemnitz, Germany
[4] Physique des Milieux Condensés, UPMC, Paris, France

Received 14 August 2002
Published online 4 February 2003 –

Abstract. We derive expressions for the intensity of the Brillouin polarized spectrum of a molecular liquid formed of axially symmetric molecules. These expressions take into account both the molecular dielectric anisotropy and the modulation of the local polarisability by density fluctuations. They also incorporate all the retardation effects which occur in such liquids. We show that the spectrum splits into a q-independent rotational contribution and q-dependent term, which reflects the propagation of longitudinal acoustic modes. In the latter, the two light scattering mechanisms enter on an equal footing and generate three scattering channels. We study the influence of the two new channels and show that they may substantially modify the Brillouin line-shape when the relaxation time of the supercooled liquid and the period of the acoustic excitation are of the same order of magnitude.

PACS. 64.70.Pf Glass transitions – 78.35.+c Brillouin and Rayleigh scattering; other light scattering – 61.25.Em Molecular liquids

1 Introduction

The theory of inelastic, low frequency, light scattering in molecular liquids has gone through different episodes over the years. The presence of a narrow inelastic doublet in the light scattering spectrum due to propagating sound waves was predicted by Brillouin in 1922 [1]. Its first observation was reported in 1930 by Gross, who noticed that the spectrum consisted of the Brillouin doublet superimposed on a central Rayleigh line [2]. An explanation of this Rayleigh-Brillouin triplet, based on the equations of macroscopic hydrodynamics, was suggested by Landau and Placzek in 1934 [3] and was given in complete form by Mountain in 1966 [4]. This hydrodynamic description did not take into account the nature of the constituents of the liquid. Yet, it can play an important role and typical molecular effects have been detected on those low frequency spectra ($\lesssim$ 50 GHz). Let us briefly mention three of them.

One takes place with molecules that are non-spherical tops. In that case, both the molecular polarisability tensor and the tensor of inertia are anisotropic and they can reasonably be considered to depend only on the molecular orientation. The (collective) orientational dynamics of the molecules can thus be detected through the corresponding fluctuations of the anisotropic part of the dielectric tensor. This corresponds to a central peak with a line shape independent both of the scattering vector and of the polarisation of the incident and scattered beams. Conversely, the tensorial character of the detection mechanism (anisotropic part of the local dielectric tensor) imposes specific relationships between the intensities of the spectra when recorded in different geometries. In particular, when, as is usually the case, dipole induced dipole effects (DID) can be neglected [5], $I_{VV}(\omega) = \frac{4}{3} I_{VH}(\omega)$. Here the first index corresponds to a vertical (V) polarisation of the incident beam, and the second index to a vertical (V) or horizontal (H) polarisation of the scattered beam, the scattering plane being horizontal.

The second effect is the possible coupling of the density fluctuations with some internal degree of freedom of the molecule, having a temperature dependent lifetime, $\tau(T)$. Although the processes involved are governed by classical mechanics and electrodynamics, we shall make use of quantum terminology. The scattering of photons is due to local rotational excitations and, depending on polarization, to longitudinal and transverse phonons. Mountain [4] showed that, when $\omega_B \tau(T) \gg 1$, where ω_B is the longitudinal phonon frequency[1], an additional central peak appears in the VV spectrum, which can be formally

[a] e-mail: franosch@hmi.de

[1] Note that, in the whole paper, we use the term 'frequency' as an abbreviation for 'circular frequency', $\omega = 2\pi\nu$.

interpreted as the introduction of a retardation effect in the bulk viscosity of the liquid.

A third effect showed up in the study of the VH spectrum of viscous molecular liquids formed of anisotropic molecules. A wave-vector dependent feature was detected, which altered the line-shape of the central peak at moderate viscosities [6] and transformed into an underdamped transverse phonon spectrum for higher viscosities [7]. It was rapidly recognised that the additional spectrum was, indeed, due to a transverse, diffusive [8], or propagative [7] excitation: any local shear motion inside the liquid couples to the mean local molecular orientation, and renders the latter anisotropic. This corresponds to a similar change of the mean molecular polarisability tensor. The detection mechanism of these shear modes is thus, as for the first effect, a change in the molecular orientations.

In addition to molecular reorientations, other light scattering mechanisms give rise to a depolarized spectrum, the most prominent being the DID mechanism. In principle, this effect alone gives rise to the effects discussed above as shown in [9]. One thus has to enter the difficult problem of estimating whether DID or the molecular anisotropy dominates the spectra. The answer depends on the system under consideration. For spherical constituents, for instance CCl_4, there is no molecular anisotropy and the depolarized spectrum is entirely due to DID effects. However, these simple liquids typically cannot be supercooled significantly. As a consequence the viscosity of such liquids remains rather low and the crossover from diffusive to propagating transverse modes cannot be observed. The glass-forming system studied in most experiments consist of molecular fluids, and rotational effects dominate as soon as some anisotropy exists [10].

To rationalise the results obtained in VH light scattering experiments, some of the present authors (C.D. and R.M.P) and co-workers, [11,12] here after referred to as [I], proposed to somewhat generalise the usual hydrodynamic equations by incorporating through phenomenological arguments, in a systematic way:

a) the coupling of the shear deformation to a local mean orientation of the molecules;
b) a retardation effect in each term corresponding to the damping of a variable.

Concentrating on the case of axially symmetric molecules, they characterised each of them by the orientation of its axis $\hat{\mathbf{u}}$, with polar angles θ, ϕ, represented by $P(\theta, \phi, \mathbf{r}, t)$ the local probability density of finding $\hat{\mathbf{u}}$ in that direction, and defined a set of orientational density variables, $Q_{ij}(\mathbf{r}, t)$ by:

$$Q_{ij}(\mathbf{r}, t) = \int \sin\theta \, \mathrm{d}\theta \, \mathrm{d}\phi P(\theta, \phi, \mathbf{r}, t) \left[\hat{u}_i \hat{u}_j - \frac{1}{3}\delta_{ij} \right], \quad (1)$$

where Latin indices $i, j, ..$ represent Cartesian components. The set of $Q_{ij}(\mathbf{r}, t)$ forms a symmetrical, traceless second rank tensor.

It was proposed in [I] that the hydrodynamic equations pertinent to the case of a such a molecular viscous liquid would consist, after linearisation, of the two conservation laws:

$$\dot{\rho}(\mathbf{r}, t) + \partial_k J_k(\mathbf{r}, t) = 0, \quad (2a)$$

$$\dot{J}_k(\mathbf{r}, t) = \partial_l \sigma_{kl}(\mathbf{r}, t), \quad (2b)$$

where $\rho(\mathbf{r}, t)$ is the mass density, $\mathbf{J}(\mathbf{r}, t)$ is the mass current density. Furthermore, they suggested the constitutive equations for the stress tensor:

$$\sigma_{ij} = (-\delta P + \eta_b \otimes \partial_k v_k)\delta_{ij} + \eta_s \otimes \tau_{ij} - \mu \otimes \dot{Q}_{ij}, \quad (3)$$

and for the orientation:

$$\ddot{Q}_{ij} = -\omega_0^2 Q_{ij} - \Gamma' \otimes \dot{Q}_{ij} + \Lambda' \mu \otimes \tau_{ij}. \quad (4)$$

Here the momentum density $\mathbf{J}$ is related to the velocity field $\mathbf{v}$ *via* the mean mass density ρ_m:

$$J_i(\mathbf{r}, t) = \rho_m v_i(\mathbf{r}, t). \quad (5)$$

The strain rate $\tau_{ij}(\mathbf{r}, t)$ is a second rank symmetric and traceless tensor defined locally by:

$$\tau_{ij} = \partial_j v_i + \partial_i v_j - \frac{2}{3}\delta_{ij}\partial_k v_k. \quad (6)$$

The pressure change $\delta P(\mathbf{r}, t)$ is related to the instantaneous mass density change $\delta\rho(\mathbf{r}, t)$ by:

$$\delta P(\mathbf{r}, t) = c^2 \delta\rho(\mathbf{r}, t)\,, \quad (7)$$

where c is the relaxed sound velocity. The retarded couplings are given in terms of η_b, η_s, μ and Γ' and are, respectively, the bulk and shear viscosities, the rotation-translation coupling and the orientational relaxation functions, the symbol $\otimes$ standing for a convolution product in time. Finally, ω_0 is the libration frequency of the axial molecules and Λ' is the rotation-translation coupling constant, a quantity that takes into account the fact that ρ and Q_{ij} have different dimensions.

Noting that, for motions that do not involve a local density change, the local dielectric tensor can be written, neglecting DID effects, as:

$$\delta\epsilon_{ij}(\mathbf{r}, t) = bQ_{ij}(\mathbf{r}, t), \quad (8)$$

it was shown in [I] that the preceding set of equations leads to an expression of the intensity that describes the complete thermal evolution of the VH spectrum of a supercooled molecular liquid.

Recently, another of the present authors (A.L.) and co-worker [13] made an additional step. Within the framework of the Molecular Mode Coupling Theory (MMCT) [14], they expressed the complete dynamics of a system of linear molecules characterised by the position of their center of mass and their orientation. They showed that, in the $\mathbf{q} \to 0$ limit, both the correlation functions of the density fluctuations and of the orientation fluctuations contributed to the light scattering mechanism in the VV geometry. This result stressed the existence of a coupling between these two variables for a longitudinal

phonon. Nevertheless, the expression they obtained for the VV intensity did not make clear two aspects. One was the separation of the intensity into a q-independent term, representing a pure rotational dynamics, and a hydrodynamic contribution. The second was that the latter could be factorized into two parts: the longitudinal phonon propagator and a phonon-photon scattering term in which both the density and the orientational fluctuations enter on an equal footing. Conversely, in another paper published soon after by two of the present authors (T.F. and A.L.) and co-workers [15], this separation into two different contributions and the emergence of several scattering channels was made apparent. Yet, the technique used in [15] did not imply any specific light scattering mechanism; it was thus not possible to predict from that paper which terms would dominate the spectrum for a given physical system.

The present series of papers aims at completing the picture of low frequency scattering in viscous molecular liquids through the combination of two different aspects. On the one hand, we shall present a full length, first principle derivation of equations (3, 4) through a Zwanzig-Mori approach and obtain from this technique the corresponding Onsager conditions which, when met by the relaxation functions, guarantee the Brillouin spectra to have a positive value whatever the frequency. On the other hand, we shall complete the results obtained in [I] by deriving, using the same phenomenological equations, expressions for the intensities which can be measured in the VV and HH scattering geometries; those are the geometries generally used to study longitudinal phonons. The results will be completely expressed with the help of the different quantities entering equations (3, 4) and a generalisation of equation (8) which includes density fluctuations.

This second series of results have immediate implications for the experimentalist and they can be derived through elementary algebraic techniques. The formal proof of the validity of the phenomenological equations and of the conditions under which the spectra are positive requires the use of more elaborate tools. In order to make the present results accessible to as large an audience as possible, we found it useful to reverse the logical order and to split our presentation into two consecutive papers. The second one (Part II) will give a complete derivation of these equations and of their consequences, only briefly sketched in [13], as well as a comparison between the results obtained through the phenomenological approach and through the more abstract technique of [15]. The phenomenological part of our work (Part I) is organised as follows.

In Section 2, we will derive the expressions for the intensity obtained in VV and HH experiments. Section 3 will discuss the changes in the line-shape of the longitudinal phonons that can be expected when the coupling of the rotation of the molecules to the longitudinal phonons is taken into account in the expression of the dielectric fluctuation. Finally, a brief summary of these results, a comparison with the expressions previously obtained for the VH intensity [I] and additional remarks will be presented in Section 4.

2 The longitudinal phonon Brillouin scattering problem

In a light scattering experiment, the incident laser may be characterised by the amplitude of the electric field E_i, and its polarization $\hat{\mathbf{e}}_i$. The spatial and temporal variation of the electric field $\mathbf{E}_\mathrm{i}(\mathbf{r},t) = E_\mathrm{i}\hat{\mathbf{e}}_\mathrm{i}\exp\mathrm{i}(\mathbf{k}_\mathrm{i}\cdot\mathbf{r}-\omega_\mathrm{i}t)$ is given in terms of the wave vector $\mathbf{k}_\mathrm{i}$ and the frequency ω_i. From the corresponding quantities of the scattered beam, $\hat{\mathbf{e}}_\mathrm{f}, \mathbf{k}_\mathrm{f}, \omega_\mathrm{f}$, one obtains insight into the fluctuations of the sample that occur at the scattering vector $\mathbf{q} = \mathbf{k}_\mathrm{i} - \mathbf{k}_\mathrm{f}$ at the frequency shift $\omega = \omega_\mathrm{i} - \omega_\mathrm{f}$. The thermal fluctuations of the dielectric tensor $\delta\epsilon_{ij}(\mathbf{r},t)$ can be decomposed into its spatial Fourier components:

$$\delta\epsilon_{ij}(\mathbf{q},t) = \int \mathrm{d}^3\mathbf{r}\ \delta\epsilon_{ij}(\mathbf{r},t)\exp(\mathrm{i}\mathbf{q}\cdot\mathbf{r}), \tag{9}$$

a notation that we will use also for other quantities for the rest of this paper. This dielectric modulation represents a momentary grating by which the laser light is scattered. Due to the polarisation of the incident beam and of the analyser for the scattered one, the detector collects only fluctuations corresponding to the projection of the dielectric fluctuations onto the two polarisations:

$$\delta\epsilon_\mathrm{fi}(\mathbf{q},t) = \hat{e}_{\mathrm{f}k}\delta\epsilon_{kl}(\mathbf{q},t)\hat{e}_{\mathrm{i}l}. \tag{10}$$

Since the fluctuations readily disappear, there is a corresponding frequency shift, ω, leading to a total scattered intensity:

$$I_\mathrm{fi}(\mathbf{q},\omega) = \int_0^\infty \mathrm{d}t\,\left\langle \delta\epsilon_\mathrm{fi}(\mathbf{q},t)\delta\epsilon^0_\mathrm{fi}(\mathbf{q})^*\right\rangle\cos(\omega t), \tag{11}$$

with the notation $\delta\epsilon^0_\mathrm{fi}(\mathbf{q}) = \delta\epsilon_\mathrm{fi}(\mathbf{q},t=0)$ and similarly for other quantities. Since in real space the fluctuations are real, one finds $\delta\epsilon^0_\mathrm{fi}(\mathbf{q})^* = \delta\epsilon^0_\mathrm{fi}(-\mathbf{q})$. Furthermore we left out well-known factors that can be found, *e.g.* in the book of Berne and Pecora [16].

In the case of longitudinal phonons, the expression for $\delta\epsilon_{ij}$ used in equation (8) is incomplete. A contribution proportional to the mass density fluctuation, $\delta\rho$, has to be added, leading to:

$$\delta\epsilon_{ij}(\mathbf{r},t) = a\delta\rho(\mathbf{r},t)\delta_{ij} + bQ_{ij}(\mathbf{r},t)\,, \tag{12}$$

where $\delta\rho$ and Q_{ij} are here the density change and its molecular orientation counterpart. Their respective spatial Fourier transforms couple dielectric fluctuations to longitudinal phonons.

Since the constitutive equations for the stress tensor and the equation of motion of the orientation are in the form of integro-differential equations it is convenient to use the Laplace-Transform (LT), which we use with the convention for functions $f(t)$:

$$LT[f(t)](\omega) = \mathrm{i}\int_0^\infty \mathrm{d}t\, f(t)\exp(-\mathrm{i}\omega t). \tag{13}$$

The scattered intensity $I_{\rm fi}(\mathbf{q},\omega)$ can thus be extracted as the imaginary part of:

$$\chi(\hat{\mathbf{e}}_{\rm i},\hat{\mathbf{e}}_{\rm f},\mathbf{q},\omega) = LT\left[\left\langle \delta\epsilon_{\rm fi}(\mathbf{q},t)\delta\epsilon^0_{\rm fi}(\mathbf{q})^*\right\rangle\right](\omega), \tag{14}$$

which defines the light-scattering problem in terms of correlation functions.

2.1 Expressions for the VV geometry

In the rest of this paper, we shall make use of the usual Berne and Pecora axes for light scattering, renamed, in agreement with [I], $\parallel$ for the direction of $\mathbf{q}$, $\perp$ for the direction perpendicular to the scattering plane, and $\perp'$ for the direction perpendicular to $\parallel$ and $\perp$. We are interested here in the usual VV scattering geometry where $\hat{\mathbf{e}}_{\rm i}$ and $\hat{\mathbf{e}}_{\rm f}$ are parallel to $\perp$ so that the r.h.s. of equation (10) reduces to $a\delta\rho + bQ_{\perp\perp}$. The expression of $\chi(\hat{\mathbf{e}}_{\rm i},\hat{\mathbf{e}}_{\rm f},\mathbf{q},\omega)$ is thus completely determined by the knowledge of the Laplace transform of the four correlation functions: $\langle\delta\rho(\mathbf{q},t)\delta\rho^0(\mathbf{q})^*\rangle$, $\langle\delta\rho(\mathbf{q},t)Q^0_{\perp\perp}(\mathbf{q})^*\rangle$, $\langle Q_{\perp\perp}(\mathbf{q},t)\delta\rho^0(\mathbf{q})^*\rangle$ and $\langle Q_{\perp\perp}(\mathbf{q},t)Q^0_{\perp\perp}(\mathbf{q})^*\rangle$, that we shall compute in turn.

The spatial Fourier transforms of equations (2a) and (2b) can be grouped into the single equation:

$$\delta\ddot{\rho}(\mathbf{q},t) = q^2\sigma_{\parallel\parallel}(\mathbf{q},t). \tag{15}$$

Inserting the constitutive equation for $\sigma_{\parallel\parallel}$, equation (3), and performing the Laplace transform yields with the help of equations (7) and (18), see below:

$$-c^2q^2\delta\rho(\mathbf{q},\omega) - q^2\mu(\omega)\left[\omega Q_{\parallel\parallel}(\mathbf{q},\omega) - Q^0_{\parallel\parallel}(\mathbf{q})\right] = \left[\frac{q^2}{\rho_m}\left[\eta_b(\omega)+\frac{4}{3}\eta_s(\omega)\right]-\omega\right]\left[\omega\delta\rho(\mathbf{q},\omega)-\delta\rho^0(\mathbf{q})\right]. \tag{16}$$

Here, we left out the term containing $\dot{\rho}^0(\mathbf{q})$ since it will drop out once correlation functions with variables of even time parity are built. Due to the coupling we also need the Fourier-Laplace transform of equation (4):

$$-\omega_0^2 Q_{ij}(\mathbf{q},\omega) - \mathrm{i}\Lambda'\mu(\omega)\tau_{ij}(\mathbf{q},\omega) = [\Gamma'(\omega)-\omega]\left[\omega Q_{ij}(\mathbf{q},\omega) - Q^0_{ij}(\mathbf{q})\right]. \tag{17}$$

As above, the term containing $\dot{Q}^0_{ij}(\mathbf{q})$ has been dropped since we will correlate equation (17) with quantities of even time parity only. Using:

$$\tau_{\parallel\parallel}(\mathbf{q},\omega) = -\frac{4}{3}\mathrm{i}qv_{\parallel}(\mathbf{q},\omega) = -\frac{4\mathrm{i}}{3\rho_m}\left[\omega\delta\rho(\mathbf{q},\omega)-\delta\rho^0(\mathbf{q})\right], \tag{18}$$

$$\tau_{\perp\perp}(\mathbf{q},\omega) = \frac{2}{3}\mathrm{i}qv_{\parallel}(\mathbf{q},\omega) = \frac{2\mathrm{i}}{3\rho_m}\left[\omega\delta\rho(\mathbf{q},\omega)-\delta\rho^0(\mathbf{q})\right], \tag{19}$$

one obtains from equation (17) for the orientational fluctuations:

$$Q_{\parallel\parallel}(\mathbf{q},\omega) = -\frac{4\Lambda'}{3\rho_m}r(\omega)\left[\delta\rho(\mathbf{q},\omega)-\delta\rho^0(\mathbf{q})/\omega\right] + \left(1-\frac{\omega_0^2}{D(\omega)}\right)\frac{Q^0_{\parallel\parallel}(\mathbf{q})}{\omega}, \tag{20}$$

$$Q_{\perp\perp}(\mathbf{q},\omega) = \frac{2\Lambda'}{3\rho_m}r(\omega)\left[\delta\rho(\mathbf{q},\omega)-\delta\rho^0(\mathbf{q})/\omega\right] + \left(1-\frac{\omega_0^2}{D(\omega)}\right)\frac{Q^0_{\perp\perp}(\mathbf{q})}{\omega}. \tag{21}$$

We have introduced, here, the quantity $D(\omega)$ which determines the frequency dependence of the pure orientational motions:

$$D(\omega) = \omega_0^2 + \omega\Gamma'(\omega) - \omega^2, \tag{22a}$$

and for later use we also introduce the rotation-translation coupling:

$$r(\omega) = \omega\mu(\omega)[D(\omega)]^{-1}. \tag{22b}$$

From equations (16, 20, 21) one can solve for orientational and density fluctuations in terms of their respective initial values:

$$\omega\delta\rho(\mathbf{q},\omega) = q^2A(\mathbf{q},\omega) + \delta\rho^0(\mathbf{q}), \tag{23}$$

$$\omega Q_{\parallel\parallel}(\mathbf{q},\omega) = \left(1-\frac{\omega_0^2}{D(\omega)}\right)Q^0_{\parallel\parallel}(\mathbf{q}) - \frac{4\Lambda' r(\omega)}{3\rho_m}q^2A(\mathbf{q},\omega), \tag{24}$$

$$\omega Q_{\perp\perp}(\mathbf{q},\omega) = \left(1-\frac{\omega_0^2}{D(\omega)}\right)Q^0_{\perp\perp}(\mathbf{q}) + \frac{2\Lambda' r(\omega)}{3\rho_m}q^2A(\mathbf{q},\omega), \tag{25}$$

with:

$$A(\mathbf{q},\omega) = P_L(q,\omega)\left[c^2\delta\rho^0(\mathbf{q}) - \omega_0^2 r(\omega)Q^0_{\parallel\parallel}(\mathbf{q})\right]. \tag{26}$$

Here $P_L(q,\omega)$ abbreviates the longitudinal phonon propagator:

$$P_L(q,\omega) = \left[\omega^2 - q^2c^2 - q^2\omega\eta_L(\omega)/\rho_m\right]^{-1}, \tag{27}$$

and, in this equation, the coupling to the parallel component of all the damping mechanisms is expressed in terms of the longitudinal viscosity:

$$\eta_L(\omega) = \eta_b(\omega) + \frac{4}{3}\left[\eta_s(\omega) - \frac{\Lambda'}{\omega}D(\omega)r(\omega)^2\right]. \tag{28}$$

The density-density and the density-orientation correlation functions are then obtained from equations (23, 24):

$$LT\left[\left\langle\delta\rho(\mathbf{q},t)\delta\rho^0(\mathbf{q})^*\right\rangle\right](\omega) = \frac{1}{\omega}\left[1+q^2c^2P_L(q,\omega)\right]\left\langle\left|\rho^0(\mathbf{q})\right|^2\right\rangle, \tag{29a}$$

$$LT\left[\left\langle\delta\rho(\mathbf{q},t)Q^0_{\perp\perp}(\mathbf{q})^*\right\rangle\right](\mathbf{q},\omega) = -q^2\frac{\omega_0^2 r(\omega)}{\omega}P_L(q,\omega)\left\langle Q^0_{\parallel\parallel}(\mathbf{q})^*Q^0_{\perp\perp}(\mathbf{q})\right\rangle, \tag{29b}$$

once one has taken into account that both $\langle|\rho^0(\mathbf{q})|^2\rangle$ and $\langle Q^0_{\parallel\parallel}(\mathbf{q})^* Q^0_{\perp\perp}(\mathbf{q})\rangle$ are of order unity, while:

$$\left\langle \delta\rho^0(\mathbf{q})^* Q^0_{\perp\perp}(\mathbf{q})\right\rangle = \left\langle Q^0_{\perp\perp}(\mathbf{q})^* \delta\rho^0(\mathbf{q})\right\rangle = \mathcal{O}(q^2 l^2), \quad (30)$$

where l is a typical intermolecular distance. The preceding relation derives from the fact that one can write, for instance:

$$\left\langle Q^0_{\parallel\parallel}(\mathbf{q})^* \rho^0(\mathbf{q})\right\rangle = \frac{m}{3N}\left\langle \sum_{\alpha=1}^{N}\sum_{\beta=1}^{N} \mathrm{e}^{\mathrm{i}\mathbf{q}\cdot(\mathbf{R}_\alpha - \mathbf{R}_\beta)}\left[3\hat{u}^2_{\parallel\beta} - 1\right]\right\rangle, \quad (31)$$

where $\mathbf{R}_\alpha$ (resp. $\mathbf{R}_\beta$) are molecular centre of mass positions and $\hat{u}_{\beta\parallel}$ is the projection of the unit vector $\hat{\mathbf{u}}$ of the molecule β on the direction $\parallel$. The exponential factor in the preceding equation can be expanded in powers of $\mathbf{q}\cdot(\mathbf{R}_\alpha - \mathbf{R}_\beta)$. One easily convinces oneself that, for symmetry reasons, the first two terms of the expansion average to zero so that the first nontrivial contribution comes from the $[\mathbf{q}\cdot(\mathbf{R}_\alpha - \mathbf{R}_\beta)]^2$ term, which is $\mathcal{O}(q^2 l^2)$. Conversely, using the same argument for the averages appearing in equations (29), one finds that the first term of the expansion already gives a nonzero value in the long-wavelength limit and is proportional to the absolute temperature. The dependence on $\mathbf{q}$ can thus be omitted in those expressions and will also be, in the rest of the paper, for all those equal-time averages.

For the VV scattering one has to study also the autocorrelation of the $\perp\perp$ component in the orientation. From equation (25) one obtains:

$$LT\left[\left\langle Q_{\perp\perp}(\mathbf{q},t)\delta\rho^0(\mathbf{q})^*\right\rangle\right](\omega) = \frac{2\Lambda'}{3\rho_m}\frac{r(\omega)}{\omega} c^2 q^2 P_L(q,\omega)\left\langle\left|\rho^0\right|^2\right\rangle, \quad (32)$$

$$LT\left[\left\langle Q_{\perp\perp}(\mathbf{q},t)Q^0_{\perp\perp}(\mathbf{q})^*\right\rangle\right](\omega) = \frac{1}{\omega}\left(1 - \frac{\omega_0^2}{D(\omega)}\right) \times \left\langle\left|Q^0_{\perp\perp}\right|^2\right\rangle - \frac{2\Lambda'}{3\rho_m}\omega_0^2\frac{r(\omega)^2}{\omega} q^2 P_L(q,\omega)\left\langle Q^0_{\parallel\parallel} Q^0_{\perp\perp}\right\rangle. \quad (33)$$

Here some comments are in order.

a) One readily verifies that, would one have taken the $\perp\perp'$ component of equation (17) instead of its $\perp\perp$ component, one would have obtained:

$$LT\left[\left\langle Q_{\perp\perp'}(\mathbf{q},t)Q^0_{\perp\perp'}(\mathbf{q})^*\right\rangle\right](\omega) = \frac{1}{\omega}\left(1 - \frac{\omega_0^2}{D(\omega)}\right)\left\langle\left|Q^0_{\perp\perp'}\right|^2\right\rangle. \quad (34)$$

Up to a b^2 factor, the imaginary part of the r.h.s. of the preceding equation is simply what is referred to as the back scattering depolarised spectrum, $I_{VH}(\omega)$, which is not sensitive to q for long wavelengths. The imaginary part of the first term of equation (33) is thus the non-acoustic part $I_{VV}(\omega)$, up to the same b^2 factor (see Eq. 12). Furthermore, since Q_{ij} is a traceless tensor of order two [16]:

$$\left\langle\left|Q^0_{\perp\perp}\right|^2\right\rangle = \frac{4}{3}\left\langle\left|Q^0_{\perp\perp'}\right|^2\right\rangle; \quad (35a)$$

the first term of the r.h.s of equation (33) represents the well-known result that the q-independent part of I_{VV} coincides with 4/3 of the back scattering spectrum $I_{VH}(\omega)$.

b) The four other terms, equations (29, 32) and the second term of the r.h.s of equation (33) all contain the phonon propagator, $P_L(q,\omega)$, and are thus q-dependent. Also, due to the spherical symmetry of the liquid:

$$\left\langle Q_{\perp\perp}(\mathbf{q},t)\delta\rho^0(\mathbf{q})^*\right\rangle = \left\langle \delta\rho(\mathbf{q},t) Q^0_{\perp\perp}(\mathbf{q})^*\right\rangle. \quad (35b)$$

Comparing equations (29b) and (32), the preceding relation implies:

$$\left\langle Q^0_{\parallel\parallel} Q^0_{\perp\perp}\right\rangle = -\frac{2\Lambda'}{3\rho_m}\frac{c^2}{\omega_0^2}\left\langle\left|\rho^0\right|^2\right\rangle, \quad (35c)$$

while, because Q_{ij} is a traceless tensor, one also has the relationship:

$$\left\langle Q^0_{\parallel\parallel} Q^0_{\perp\perp}\right\rangle = -\frac{1}{2}\left\langle\left|Q^0_{\parallel\parallel}\right|^2\right\rangle. \quad (35d)$$

Inserting these results into equations (11, 12), one finally obtains for the intensity in a VV scattering experiment:

$$I_{VV}(q,\omega) = \frac{\langle|Q^0_{\perp\perp'}|^2\rangle}{\omega}\mathrm{Im}\left\{\frac{4b^2}{3}\left[1 - \frac{\omega_0^2}{D(\omega)}\right] + \frac{\rho_m}{\Lambda'}(\omega_0 q)^2 P_L(q,\omega)\left[a + \frac{2\Lambda'}{3\rho_m} b r(\omega)\right]^2\right\}, \quad (36)$$

where the preceding formula makes clear that the first term is 4/3 the $I_{VH}(\omega)$ back scattering spectrum.

The preceding results call for two remarks.

a) Equation (35c) simply expresses the equipartition of energy between the centre of mass motions and the libration motions:

$$\frac{3\omega_0^2}{4\Lambda'}\left\langle\left|Q^0_{\parallel\parallel}\right|^2\right\rangle = \frac{c^2}{\rho_m}\left\langle\left|\rho^0\right|^2\right\rangle \propto k_B T, \quad (37)$$

and this is a necessary condition for the consistency of the phenomenological theory summarised in Section 1. Equation (37) will appear in a natural way in the microscopic derivation of the phenomenological equations (see Eqs. (30c, 31b) of Part II).

b) Equation (36) completes previous results obtained in [13], separating clearly the role of the phonon propagator, $P_L(q,\omega)$ from that of the scattering mechanisms (a and b, with appropriate factors). It also separates the non-hydrodynamic, rotational contribution (first term of Eq. (36)) from the hydrodynamic one. In the latter, one part (term in b^2) is entirely due to scattering by the anisotropic part of the polarisability tensor of the molecules. The same mechanism was at the origin of the

q-dependent part of $I_{VH}(q,\omega)$ in [I] and in both cases the scattered intensity is proportional to a phonon propagator, longitudinal or transverse, multiplied by the same $r(\omega)^2$ factor; the power two stresses that the molecular orientation acts twice, once as the source of the fluctuation and, the second time, as the detection mechanism. The more complex form obtained here for the q-dependent part of $I_{VV}(q,\omega)$ is the direct consequence of the existence of two parallel channels, $\delta\rho$ and Q_{ij}, in the case of longitudinal phonons; this is in contradistinction with the single channel case of the transverse phonons [I].

2.2 Results for the HH geometry

The same technique can be used to derive the intensity which can be obtained in an HH experiment; indeed in such a case:

$$\delta\epsilon_{HH}(\mathbf{q},t) = \delta\epsilon_{\perp'\perp'}(\mathbf{q},t)\sin^2\frac{\theta}{2} - \delta\epsilon_{\parallel\parallel}(\mathbf{q},t)\cos^2\frac{\theta}{2}, \quad (38)$$

where θ is the scattering angle. Expanding in terms of density and orientation, one has to consider:

$$\delta\epsilon_{HH}(\mathbf{q},t) = -a\delta\rho(\mathbf{q},t)\cos\theta + bQ_{\perp'\perp'}(\mathbf{q},t)\sin^2\frac{\theta}{2} - bQ_{\parallel\parallel}(\mathbf{q},t)\cos^2\frac{\theta}{2}\cdot \quad (39)$$

To calculate the corresponding auto-correlation function as required by equation (11), one needs again the dynamics of density and orientation. Repeating the calculations of Section 2.1, one convinces oneself that equation (25) remains valid if $\perp\perp$ is replaced by $\perp'\perp'$. Due to rotational symmetry, the cross correlators are again identical as in equation (35b). Of the six correlation functions that can be built in equation (39), one can easily compute the missing three by the methods of the preceding subsection. From equation (24), one finds:

$$LT\left[\left\langle Q_{\parallel\parallel}(\mathbf{q},t)Q^0_{\perp'\perp'}(\mathbf{q})^*\right\rangle\right](\omega) = \left\{\left(1-\frac{\omega_0^2}{D(\omega)}\right) + \frac{4\Lambda'\omega_0^2}{3\rho_m}r(\omega)^2q^2P_L(\mathbf{q},\omega)\right\}\frac{\left\langle Q^0_{\parallel\parallel}Q^0_{\perp'\perp'}\right\rangle}{\omega}, \quad (40)$$

$$LT\left[\left\langle Q_{\parallel\parallel}(\mathbf{q},t)Q^0_{\parallel\parallel}(\mathbf{q})^*\right\rangle\right](\omega) = \left\{\left(1-\frac{\omega_0^2}{D(\omega)}\right) + \frac{4\Lambda'\omega_0^2}{3\rho_m}r(\omega)^2q^2P_L(\mathbf{q},\omega)\right\}\frac{\left\langle \left|Q^0_{\parallel\parallel}\right|^2\right\rangle}{\omega}, \quad (41)$$

$$LT\left[\left\langle Q_{\parallel\parallel}(\mathbf{q},t)\delta\rho^0(\mathbf{q})^*\right\rangle\right](\omega) = -\frac{4\Lambda'c^2}{3\rho_m}r(\omega)q^2P_L(\mathbf{q},\omega)\frac{\left\langle \left|\delta\rho^0\right|^2\right\rangle}{\omega}\cdot \quad (42)$$

Collecting all the terms appearing in equations (14, 39) with $\delta\epsilon_{\text{fi}} = \delta\epsilon_{HH}$, one arrives at our final expression for the HH scattering spectrum:

$$I_{HH}(q,\omega) = \frac{\left\langle \left|Q^0_{\perp\perp'}\right|^2\right\rangle}{\omega}\left\{\frac{4b^2}{3}\left(1-\frac{1}{4}\sin^2\theta\right)\left[1-\frac{\omega_0^2}{D(\omega)}\right] + \frac{\rho_m\omega_0^2}{\Lambda'}q^2P_L(q,\omega)\left[a\cos\theta - \frac{b\Lambda' r(\omega)}{3\rho_m}(3+\cos\theta)\right]^2\right\}. \quad (43)$$

For a given $\mathbf{q}$, all other scattering geometries give intensities, which are linear combinations of $I_{VV}(q,\omega)$ and $I_{HH}(q,\omega)$ as well as of $I_{VH}(q,\omega)$, whose q-dependent part detects the transverse phonon, whereas the q-independent part detects again $I_{VH}(\omega)$, equation (34). It is thus not possible to detect independently the contributions of the three terms entering, *e.g.* equation (36). Equations (36) and (43) are very compact expressions in which the q-dependent and the q-independent parts have been separated. They allow to study, within some approximations for the different quantities entering them, the influence of the rotation-translation coupling on the shape of a typical longitudinal phonon spectrum. Using for those quantities the same toy model as in [13], we shall proceed to this comparison in the next section.

3 Analytical and numerical discussion

3.1 Introduction

In this section, we discuss some typical features of the spectra obtained in a VV scattering experiment. As we shall see, the rotation-translation coupling gives rise to spectra which differ in shape and, more importantly, in some cases in the values for the relaxation times, would they be extracted from the widely used model where density fluctuations are considered as the sole light scattering mechanism for the q-dependent part of the polarized spectrum, *i.e.*:

$$I^{single}_{VV}(q,\omega) = \frac{4}{3}I_{VH}(\omega) + \frac{a^2c^2q^2}{\omega}\left\langle\left|\rho^0\right|^2\right\rangle \mathrm{Im}P_L(q,\omega). \quad (44)$$

In order to demonstrate the effects which take place when translation-rotation coupling is non-negligible, we generate data for the q-dependent part of a VV experiment by using the full expression, equation (36). The spectral shape is then determined by the frequency dependence of the four fundamental memory kernels $\eta_s(\omega), \eta_b(\omega), \mu(\omega)$ and $\Gamma'(\omega)$. To keep the discussion as simple as possible, we shall model the relaxation kernels by single exponential Debye processes:

$$M(\omega) = \Delta_M^2\frac{\mathrm{i}\tau}{1+\mathrm{i}\omega\tau}, \quad (45)$$

where M is any of η_s, η_b, μ or Γ'. Once the spectra have been generated, we treat them as raw data and analyse them by a 'density-only' model, equation (44), in which, see equation (27), $\omega_L = cq$ and $\eta_L(\omega)$ have to be fitted; in the spirit of the simplifying assumptions made above, $\eta_L(\omega)$ is also a simple Debye process, characterised as in equation (45), by an amplitude, Δ_L^2, and a fitted relaxation time, τ_L.

Let us first make some comments on the general shape of the spectra. For a given wave vector $\mathbf{q}$, the second part of the r.h.s of equations (36 or 43) is the sum of three terms that correspond to three channels of detection of the longitudinal phonons: a density-only channel, proportional to a^2, an orientation-only one ($\propto b^2$) and a cross channel of density and orientation ($\propto ab$). For a simple liquid, the first one is predominant, which depends solely on $P_L(q,\omega)$ and the shape of the corresponding spectrum has been studied in detail, in particular for supercooled liquids, in many papers [17–21]. The purpose of these papers was basically to extract information on the memory function $\eta_L(\omega)$, and on its dependence on temperature. In particular, if $\eta_L(\omega)$ is characterised by a single Debye relaxation process with a relaxation time τ_L and an amplitude such that, whatever τ_L, $\mathrm{Im}P_L(q,\omega)/\omega$ exhibits a well-defined peak, the density spectrum varies in a specific manner with τ_L: for $\omega_B\tau_L \ll 1$, with $\omega_B = cq$, the spectrum contains a quite narrow Brillouin peak centered around, say ω_{B1}, with a weak background for other frequencies. The same is true for $\omega_B\tau_L \gg 1$, but the peak is now centered at $\omega_{B2} \gg \omega_{B1}$. The only regime where a rather precise information on τ_L is obtained occurs for $\omega_B\tau_L \sim 1$, *i.e.* approximately $1/5 \lesssim \omega_B\tau_L \lesssim 5$.

The influence of the orientation-only channel on the shape of the q-dependent part of the VV spectrum was discussed in [13], with the help of a similarly simple model for the four relaxation kernels; conversely, the cross channel ($\propto ab$) was not studied in that paper. We will thus first compare the shape of the contributions of the three channels. We shall then discuss the line-shape of the total q-dependent part of the VV spectrum, focusing mostly on the $\omega_B\tau \sim 1$ regime. To remain as close as possible to the results presented in [13], we take the same numerical values for the various temperature independent parameters, $c = 0.6, q = 0.02, \omega_0 = 1$, the units being chosen such that $\Lambda' = 1$ and $\rho_m = 1$. In order to restrict the number of parameters, the relaxation time τ is the same for all four memory kernels indicated in equation (45), and we use the same values of τ as in [13], simply studying also and in more details the $\omega_B\tau \sim 1$ regime. The amplitudes are taken as $\Delta_{\eta_b} = 1/\sqrt{2}, \Delta_{\eta_s} = \sqrt{3/8}$ and $\Delta_\mu = \sqrt[4]{3/16}$ in order to use the same phonon propagator as in [13]. Since the Brillouin peak is at much smaller frequencies than the libration frequency, ω_0, the spectra are not sensitive to the value of $\Delta_{\Gamma'}$ in the frequency window studied here. Hence, we set $\Delta_{\Gamma'} = 0$, or $\Gamma'(\omega) \equiv 0$. Finally, one needs a plausible numerical value for the ratio $2\Lambda' a/3\rho_m b$. Its estimate can be obtained from the following considerations. Impulsive Stimulated Thermal Scattering (ISTS) experiments have been performed on supercooled liquids formed of anisotropic molecules such as salol and OTP. It has been recognised recently that the spectral shape of the signal obtained in this pump-probe experiment is sensitive to the polarisation of the probe beam [22,23]. In these experiments, the origin of the signal is not the thermal fluctuations of $\delta\rho$ and Q_{ij} but the intensity of the pump beam; conversely, the signal is detected through the dependence of the local dielectric tensor on density and orientation as in a VV experiment. The ISTS signal then turns out to be linear in $\delta\rho$ and Q_{ij} with the same coefficients as in equation (36). Making use of different polarisations of the probe beam, the contribution of the two variables can be disentangled [22], and a value for a typical molecular liquid, metatoluidine, of the order of 0.5 can be derived from the results of [22]. In order to overemphasise the effect of the additional scattering channels, we have found it convenient, in the present paper, to choose a value equal to $4/\sqrt{27} \approx 0.77$. All the results presented in this section have been obtained with those numerical values.

3.2 Analysis of the role of the two additional channels

3.2.1 The $\omega_B\tau \ll 1$ and the $\omega_B\tau \gg 1$ regimes

– Preliminary remarks

As already alluded in 3.1 of this section, the two regimes $\omega_B\tau \ll 1$ and $\omega_B\tau \gg 1$ are rather uninteresting from the practical point of view of determining a value of τ: the most important piece of information is contained in the position of the Brillouin peak, its linewidth being much more difficult to analyse because its exact line-shape cannot be determined. The remaining low intensity part of the Brillouin line cannot be studied experimentally because it cannot be disentangled, either from the wing of the central peak (first term of the r.h.s of Eq. (36)) for high temperatures, *i.e.* $\omega_B\tau \ll 1$, or from a flat background for low temperature, $\omega_B\tau \gg 1$. Let us just mention here that, even in these regimes, at very low frequency, the r.h.s of the second term of equation (36) can lead to a negative contribution to the intensity, due to the existence of the $r(\omega)$ and $r(\omega)^2$ terms, as was already mentioned for the latter case in [13]. This is not an artefact of the theory, equations (3, 4, 12), but a consequence of the introduction of translation-rotation coupling into these equations. If one takes it into account, it is no longer necessary that the q-dependent part of equation (36) is always positive, the requirement being that only the full r.h.s of this equation is positive. We shall defer the discussion of this point to Section 4 and, mostly, to Part II [24].

In spite of the preceding remark on the δ-like shape of those spectra in the two regimes, their study turns out to be instructive, because the way the two additional channels contribute to the spectrum will be similar in the $\omega_B\tau \sim 1$ regime we shall study later; there, one will directly detect their influence on the line-shape while their analytical study is easier in the extreme cases we consider here. We shall first develop analytic formulae, then demonstrate that these effects do show up in the line-shape of the $\mathrm{Im}[r(\omega)P_L(q,\omega)/\omega]$ and $\mathrm{Im}[r(\omega)^2P_L(q,\omega)/\omega]$

Table 1. Analytic form for the different scattering channels in the two limiting cases. The first line, a^2, gives the analytic form of $\mathrm{Im}[P_L(q,\omega)/\omega]$ for $\omega \ll \omega_B$, at the peak value and for $\omega \gg \omega_B$, for the two cases $\omega_B\tau \ll 1$ and $\omega_B\tau \gg 1$. The last four lines give the factors by which the first line has to be multiplied to obtain the analytical form of the corresponding term; the factors are given for the b^2 channel (second and third lines) and for the ab channel (fourth and fifth lines). In both cases, the two terms, R(eal) I(maginary) and I(maginary)R(eal), are given in the even, respectively odd, lines (see Eq. (46)).

	$\omega_B\tau \ll 1$			$\omega_B\tau \gg 1$		
	$\omega \ll \omega_B$	Brillouin peak	$\omega \gg \omega_B$	$\omega \ll \omega_B$	Brillouin peak	$\omega \gg \omega_B$
a^2	$\frac{\Delta^2\tau}{q^2c^4}$	$\frac{1}{\Delta^2q^3c\tau}$	$\frac{q^2\Delta^2\tau}{\omega^4}$	$\frac{\Delta^2}{\omega^2\tau^2q^2(c^2+\Delta^2)^2}$	$\frac{\tau}{q^2\Delta^2}$	$\frac{q^2\Delta^2}{\omega^6\tau}$
b^2 RI	$-(\omega\tau)^2$		$-(\omega\tau)^2$	1		1
b^2 IR	$-(\omega\tau)^2\frac{c^2}{\Delta^2}$		$(\omega\tau)^2\frac{\omega^2}{q^2\Delta^2}$	$-\frac{c^2+\Delta^2}{\Delta^2}$		$\frac{\omega^2}{q^2\Delta^2}$
ab RI	$-(\omega\tau)^2$		$-(\omega\tau)^2$	1		1
ab IR	$-\frac{c^2}{\Delta^2}$		$\frac{\omega^2}{q^2\Delta^2}$	$-\frac{c^2+\Delta^2}{\Delta^2}$		$\frac{\omega^2}{q^2\Delta^2}$

spectra, if analysed with sufficiently large accuracy, and finally show that, nevertheless, the q-dependent part of the VV spectrum is little affected by these effects in the two cases, $\omega_B\tau \ll 1$ and $\omega_B\tau \gg 1$, in the region of the Brillouin peak.

– Analytical results

Table 1 displays the analytical form of the leading terms for the three channels, *viz.* pure density (a^2), pure rotation (b^2) and cross channel (ab), both for $\omega \ll \omega_B$ and $\omega \gg \omega_B$; for the sake of completeness, the table also displays the approximate Brillouin peak intensity related to the first channel. In order to make this table as easy to read as possible, the quantities for the b^2 and ab channels are the factors by which the results of the first line (a^2 channel) have to be multiplied in order to obtain the corresponding contribution to the intensity.

Furthermore, while the intensity of the pure density channel is simply equal to $\mathrm{Im}[P_L(q,\omega)/\omega]$, in the case of the pure orientation channel for instance, its intensity $I_{b^2}(\omega)$ is given by:

$$\frac{1}{\omega}\mathrm{Im}[r(\omega)^2P_L(q,\omega)] = \frac{1}{\omega}\left\{\mathrm{Re}\left[r(\omega)^2\right]\mathrm{Im}\left[P_L(q,\omega)\right] + \mathrm{Im}[r(\omega)^2]\mathrm{Re}[P_L(q,\omega)]\right\}, \quad (46)$$

and a similar expression holds for the cross channel. Since $\mathrm{Im}[P_L(q,\omega)/\omega]$ has typical functional form $[1+X^2]^{-1}$ with $X = \omega - \omega_B$ for $\omega > 0$, the corresponding real part $\mathrm{Re}[P_L(q,\omega)/\omega]$ is described by $X/[1+X^2]$; the contributions of the two terms of equation (46), and similar terms in the ab channel, have different line-shapes and have to be considered separately. They are denoted as RI and IR contributions in the lower part of Table 1. Finally, we simplified our study by admitting that, in the limited frequency range for which this table is constructed, $\omega_B/10 \lesssim \omega \lesssim 10\omega_B$, the dimensionless quantities $\omega\tau$ and $\omega_B\tau$ have always the same order of magnitude. Table 1 shows that one has to study three different cases:

a) $\omega_B\tau \gg 1$
Within the approximation just mentioned, the b^2 and the ab channels have the same multiplying factors, and their RI parts give rise to exactly the same line-shape as the a^2 channel. For $\omega \gg \omega_B$, the $(\omega/q\Delta)^2$ factor of the IR term increases the intensity with respect to the a^2 channel; conversely, for $\omega \ll \omega_B$, the same IR term gives a negative contribution: the relative intensities will be lower than in the a^2 channel.

b) $\omega_B\tau \ll 1$
– The b^2 channel has a general $(\omega\tau)^2$ factor which renders its contribution small on the whole frequency domain whatever its sign. The IR part gives a negative contribution for $\omega < \omega_B$ which changes into a positive one at some value above ω_B, while the RI part always remains negative.
– The ab channel gives a line-shape quite different from the ones discussed above since it is dominated by its IR part with a prefactor of order unity while the RI part is suppressed by a factor of $(\omega\tau)^2$. This results into a typical $X/[1+X^2]$ line shape with a negative contribution for $\omega < \omega_B$, a minimum below ω_B, a zero in the vicinity of ω_B, and a positive contribution above ω_B, the maximum of the latter being slightly above ω_B.

– Numerical results

Figures 1, 2 and 3 illustrate the preceding results. Figure 1 displays the intensity related to b^2 channel, I_{b^2}, for $\tau = 1, 10^2, 10^3$ and 10^5. The crossover regime $\omega_B\tau \sim 1$ corresponds to $\tau \sim 10^2$. The different curves exhibit the shapes discussed above. Note that for clarity the spectrum corresponding to $\tau = 1$ has been enhanced by a factor of 100. Yet, the spectra for $\omega_B\tau \gg 1$ exhibit an additional, strongly negative feature for $\omega \ll \omega_B$, which was not studied in Table 1, as it is related to the $\omega\tau \ll 1$ part of these spectra.

The different shapes of the I_{ab} spectra are shown in Figure 2. These shapes agree with what can be inferred, in the $\omega_B\tau \gg 1$ and $\omega_B\tau \ll 1$ regimes, from the results shown in Table 1.

Finally, Figure 3 represents the ratio of the total q-dependent part of I_{VV}, equation (36), called I_{tot}, to the a^2 channel intensity alone, I_{a^2}. Here the two spectra are

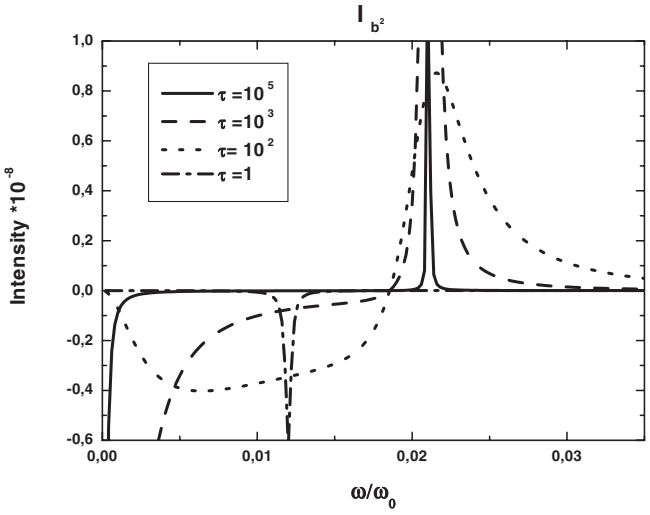

Fig. 1. The intensity of the orientation-only channel I_{b^2} for four values of τ: $\tau = 1, 10^2, 10^3$ and 10^5. The spectrum for $\tau = 1$ has been multiplied by 100 to make it visible on the same figure.

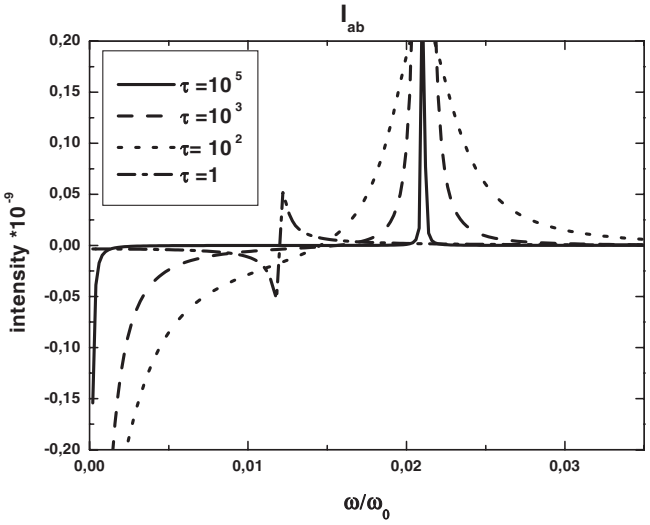

Fig. 2. The intensity of the cross channel I_{ab} for the same values of τ as in Figure 1. The shape of the $\tau = 1$ spectrum differs strongly from the remaining ones.

normalised to the same intensity at the Brillouin peak. The factor $(\omega/q\Delta)^2$, general to the IR part for $\omega \gg \omega_B$, explains the increase of the ratio in this frequency domain, a signature that will remain also in the $\omega_B\tau \sim 1$ regime. Also, this ratio always decreases, more or less strongly, below ω_B due to the negative value of the same term in this frequency range. This effect also shows up in the $\omega_B\tau \sim 1$ regime, as can be inferred from Figure 3 for the curve corresponding to $\tau = 10^2$. Conversely, one observes that the ratio is close to unity for frequencies in the vicinity of ω_B. As long as $\omega_B\tau \gg 1$ or $\omega_B\tau \ll 1$, the shape of the Brillouin line of the total q-dependent part of I_{VV} is indistinguishable from that of the pure density channel. Hence, one needs to analyse the $\omega_B\tau \sim 1$ regime to detect a difference

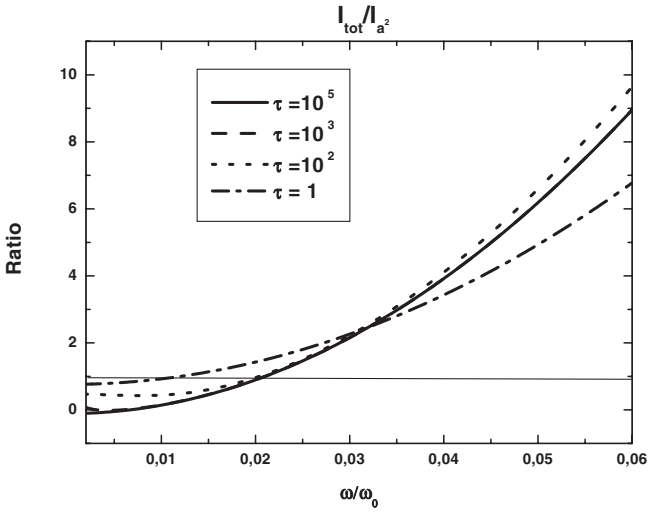

Fig. 3. The ratio of KI_{tot} to I_{a^2} for the same values of τ as in Figure 1. For each spectrum, K is adjusted in a such a way that the intensities of the two spectra are identical at the Brillouin peak. The horizontal line, drawn for a ratio equal to 1, allows to locate these Brillouin peaks for the four cases.

between the 'density-only' and the 'density+orientation' scattering model.

3.2.2 Numerical analysis of the $\omega_B\tau \sim 1$ regime

In order to look for an experimentally detectable effect, we have computed the total q-dependent part of the intensity, I_{tot}, for the 10 values of τ reported in the first column of Table 2, all close to the $\omega_B\tau \sim 1$ condition. Those 10 spectra are shown in Figure 4 as dashed lines and we have checked that they notably differ from the scaled spectra that can be obtained for the same values of τ considering a line-shape as given by equation (44). To explore more closely the effect of the additional channels, both on the line shape and on a possible misinterpretation of these spectra in terms of 'density-only' spectra, we have tried to fit them with a $\mathrm{Im}[P_L(q,\omega)/\omega]$ expression, where the longitudinal viscosity was expressed as:

$$q^2\omega\eta_L(\omega)/\rho_m = \Delta_L^2 \frac{\mathrm{i}\omega\tau_L}{1+\mathrm{i}\omega\tau_L} + \mathrm{i}\omega\gamma_L. \qquad (47)$$

A value of γ_L, consistent with a previous Brillouin scattering study of m-toluidine [19], $\gamma_L = 10^{-5}$, was chosen, and fits for the spectra corresponding to the ten different values of τ were performed, treating $\Delta_L, \omega_L = cq$ and τ_L as free parameters.

The numerical values extracted from the best fits, as well as the value of the peak frequency of I_{tot}, ω_B, are reported in Table 2. The fits are displayed in Figure 4 and they show that the closer $\omega_B\tau$ is to unity, the worse is the agreement with the density-only model. Note that the value of $2\Lambda' a/3\rho_m b$ has been overestimated to emphasize the effect. The discrepancy between the fit function and the computed spectra has always the characteristic

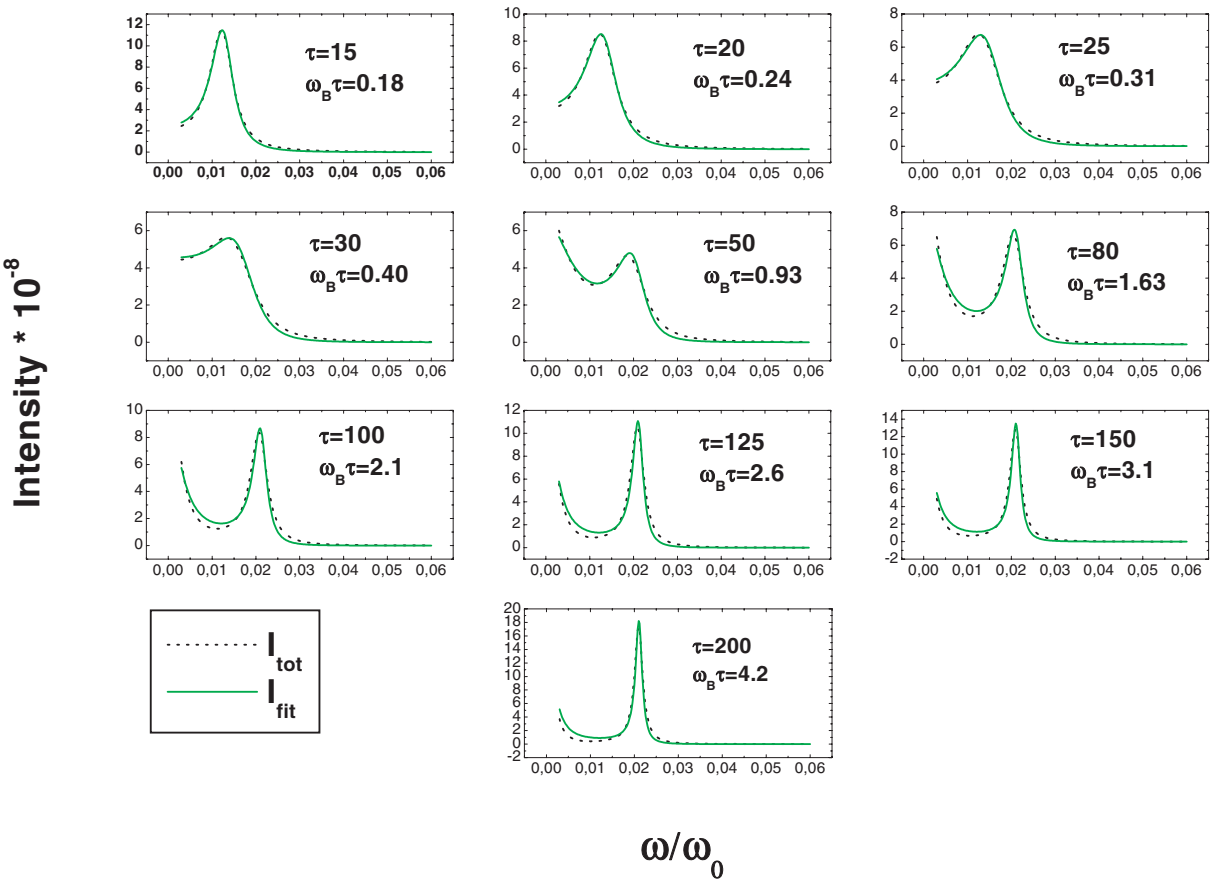

Fig. 4. I_{tot} (dashed line) for 10 values of τ in the vicinity of $\omega_B\tau = 1$, and its fit (full line) with a I_{a^2} model (see text). The values of τ and $\omega_B\tau$ are indicated in each case.

Table 2. Fit parameters of the total spectrum for 10 different values of τ. The first column gives the values of τ for which the total spectra, I_{tot}, are computed. The three next columns give the fit values for τ_L, Δ_L (see Eq. (47)) and ω_L, the relaxed phonon frequency, while the last one gives the frequency, ω_B, of the peak of I_{tot}. Note that, for these values of τ, I_{tot} exhibits a broad enough maximum (see Fig. 4) for ω_B to be defined with an uncertainty of order 5×10^{-4}.

τ [a]	τ_L [b]	Δ_L [b]	ω_L [b]	ω_B [c]
15	13.4	0.0210	0.0125	0.0121
20	19.8	0.0200	0.0128	0.0123
25	27.6	0.0190	0.0131	0.0125
30	37.0	0.0180	0.0133	0.0132
50	67.7	0.0170	0.0141	0.0186
80	109	0.0160	0.0147	0.0204
100	136	0.0156	0.0149	0.0207
125	175	0.0154	0.0148	0.0208
150	209	0.0152	0.0149	0.0210
200	270	0.0150	0.0150	0.0210

[a] initial value
[b] fitted value
[c] deduced from $I_{tot}(\omega)$.

features discussed before: the fit function has a lower intensity than the computed one above the Brillouin peak and a higher one below.

The trends reported in Table 2 are worth commenting: the ratio τ_L/τ increases with longer relaxation times τ, *i.e.* lower temperatures: the apparent relaxation time τ_L is longer than the original one. In Brillouin experiments on supercooled liquids, this effect will take place for relaxation times of the order of some nanoseconds, while it cannot be identified for much longer relaxation times. The effect will then be apparent in the region where the curve $\log\tau$ *versus* $1/T$ has its maximum curvature for fragile glass forming liquids. This curvature is the origin of the nonzero value of the Vogel-Fulcher temperature: an apparent increase of the relaxation times in this time window will decrease this curvature and result in an artificial decrease of the Vogel-Fulcher temperature.

Table 2 also exhibits an effect that has not been reported in experimental studies of Brillouin spectra of supercooled liquids: a decrease, instead of an increase, of Δ_L upon cooling [17–21]. This contrasts with the familiar trend of ω_L which increases with τ as is shown in Table 2. The unconventional dependence on temperature of Δ_L may be an artefact of the oversimplified model for the memory kernels.

4 Summary and final remarks

The present paper aimed at giving complete and transparent expressions for polarised Brillouin light scattering experiments within the framework of the phenomenological equations recalled in the Introduction. These equations have been derived through the use of heuristic arguments in [I] and a demonstration of their validity has been briefly sketched in [13]. Their detailed proof will be given in the second paper of this series (Part II), where the same set of relevant variables, *i.e.* mass density ρ, orientation Q_{ij} and their respective currents are considered.

The expressions for the intensity in the VV and HH scattering geometry are given by equations (36) and (43). In both cases, the spectrum naturally splits into a sum of two terms: one describes the pure orientational dynamics of the molecules, decoupled from density fluctuations; the second term involves the propagation of longitudinal phonons. The corresponding longitudinal viscosity comprises contributions from the relaxation of the translational and orientational motions. The coupling of these two types of motion is characterised by the translation-rotation coupling constant, Λ', and by the frequency-dependent rotation-translation function, $\mu(\omega)$, while the orientational dynamics is characterised by $D(\omega)$ which depends very weakly on ω in the region of interest for Brillouin scattering studies. The role of Λ' and $r(\omega)$ in the spectra is twofold: first, their play a role in the phonon propagator and, second, they enter in the detection mechanism *via* the factor $[a + 2\Lambda' br(\omega)/3\rho_m]$.

The role of the molecular polarisability anisotropy in detecting both the uncoupled orientational dynamics and the transverse, diffusive or propagative modes with wave vector $\mathbf{q}$ already appeared in [I]. For the sake of completeness, we reproduce here the results obtained in that paper under a from that allows for an easy comparison with equation (36):

$$I_{VH}(q,\omega) = \frac{\left\langle \left| Q^0_{\perp\perp'} \right|^2 \right\rangle}{\omega} \mathrm{Im} \Bigg\{ b^2 \left[1 - \frac{\omega_0^2}{D(\omega)} \right] + \frac{\rho_m}{\Lambda'} (\omega_o q)^2 \cos^2 \frac{\theta}{2} P_T(q,\omega) \left[\frac{\Lambda'}{\rho_m} br(\omega) \right]^2 \Bigg\}, \quad (48)$$

where the q-dependent part is now mediated by the transverse phonon propagator:

$$P_T(q,\omega) = \left[\omega^2 - q^2 \rho_m^{-1} \omega \eta_T(\omega) \right]^{-1}, \quad (49)$$

characterised by the transverse viscosity:

$$\eta_T(\omega) = \eta_s(\omega) - \frac{\Lambda'}{\omega} D(\omega) r(\omega)^2. \quad (50)$$

The absence, in the second square bracket of equation (48) of the factor 2/3 is in agreement with a result of [15], as will be discussed in Part II.

We studied, in Section 3, the change in the spectral line-shape brought by taking into account the additional light scattering channels. We concentrated on the second term of the r.h.s. of equation (36), mostly discussing the type of distortion produced by these new terms in the spectral shape in the vicinity of the Brillouin peak. Let us add some remarks.

Firstly, in Section 3, the numerical calculation of the total intensity was performed using a positive ratio b/a and we assumed through equation (44) that $\mu(t)$ could be characterised by some amplitude, Δ_μ^2, and a smooth, positive, decreasing function of time that approaches zero for long times. Contrary to the coefficient a in equation (12), the numbers b and Δ_μ^2 are not always positive, but we want to point out that their product $b\Delta_\mu^2$ is commonly a positive quantity, for prolate as well as for oblate axial molecules. Indeed, on the one hand, the polarisability anisotropy, b, is usually positive for prolate molecules giving rise to glass-forming liquids and negative for the oblate ones. On the other hand, the sign of $\mu(t)$ is also shape dependent as can be inferred from the following argument. Subjected to a steady shear flow, τ_{ij}, a molecular liquid builds up a nonzero stationary mean orientation Q_{ij} which is easily deduced from equation (4):

$$Q_{ij} = \frac{1}{\omega_0^2} \left[\int_0^\infty \mu(t) \mathrm{d}t \right] \tau_{ij}. \quad (51)$$

If, for instance, this flow is in the $\hat{\mathbf{x}}$ direction with a positive gradient in the $\hat{\mathbf{z}}$ direction, *i.e.* $\tau_{xz} > 0$, one easily convinces oneself that a long axis of the molecule will be, on average, parallel to $\hat{\mathbf{x}} + \hat{\mathbf{z}}$, and a short axis parallel to $\hat{\mathbf{x}} - \hat{\mathbf{z}}$. Hence, cigar-shaped molecules will exhibit $Q_{xz} > 0$, whereas disk-shaped ones lead to $Q_{xz} < 0$. In other words, the shear flow exerts a torque on the molecules so that the sign of:

$$\int_0^\infty \mu(t) \mathrm{d}t = \mathrm{Im}\mu(\omega = 0), \quad (52)$$

which is also the sign of Δ_μ^2 for a smoothly decreasing function $\mathrm{Im}\mu(\omega)$, is the same as the sign of b.

Secondly, the total VV spectrum is the sum of two terms in equation (36): the first is proportional to the backscattering VH spectrum and gives always a positive contribution to the intensity for all frequencies. Conversely, at very low frequencies, the second, q-dependent, term may give rise to a negative contribution. This is in contrast to the density-only model and may serve as a simple test to determine whether or not translation-orientation coupling is significant. Since the measured spectrum should be positive whatever the frequency, one would like to know if the proposed phenomenological equations ensure this property and, if necessary, what additional requirements have to be imposed on the memory kernels to guarantee this positiveness. The phenomenological equations allow to derive the appropriate conditions. However, these conditions will appear more naturally and in a transparent way in the microscopic approach. Therefore their derivation will be postponed to Part II and

we merely state here the result: the measurable spectra in the three geometries VV, HH, VH, equations (36, 43) and (48), are positive for all frequencies provided that:

a) the imaginary part of $\Gamma'(\omega), \eta_b(\omega)$ and $\eta_s(\omega)$ are positive for all frequencies;
b) the imaginary part of the translation-rotation coupling fulfills:

$$[\mathrm{Im}\Gamma'(\omega)][\mathrm{Im}\eta_s(\omega)] - \Lambda'[\mathrm{Im}\mu(\omega)]^2 > 0. \qquad (53)$$

This conditions appear as a generalisation of the Onsager relations for the dynamics of a coupled system and are, as expected, independent of the a/b ratio. This corroborates the argument that the positiveness of the spectra should not depend on the relative strength of the two scattering mechanisms. In view of the analytical form of the memory kernels as given in equation (44), and with the numerical values used in Section 3 for $\Delta_{\eta_b}, \Delta_{\eta_s}, \Delta_\mu$ and Λ', equation (53) is fulfilled for all frequencies if $\Delta^2_{\Gamma'} > 1/2$. Nevertheless, in the frequency range considered, the role of $\Delta_{\Gamma'}$ is important only in the q-independent part of equation (36) (rotational part of the spectrum):

$$\frac{1}{\omega}\mathrm{Im}\left[1 - \frac{\omega_0^2}{D(\omega)}\right] = \frac{1}{\omega}\mathrm{Im}\left[\frac{\omega\Gamma'(\omega) - \omega^2}{D(\omega)}\right]. \qquad (54)$$

We have checked that the neglect of $\Delta_{\Gamma'}$ in $D(\omega)$, both in the denominator of the r.h.s. of equation (54) and in $r(\omega)$, has virtually no influence: it does not change the intensity and the shape, either of the pure rotational spectrum, or of the q-dependent spectrum discussed in Section 3. Conversely, this neglect allows for the analytic discussion of I_{tot} performed in that section. This justifies, a posteriori, the simplification made there.

Finally, we already pointed out in the Introduction that effects related to energy conservation, in particular to thermal diffusion, are neglected in the present paper. Some consequences of the heat diffusion process are well known since the pioneer work of Landau and Placzek [3]. It gives rise to contributions in the propagator of longitudinal phonons for very low frequencies. Other aspects of the role of temperature fluctuations were taken into account in [15]. There, it was shown that, if one deals explicitly with the coupling of temperature to dielectric fluctuations, one arrives at a rather complex form of the coupling of detection channels and propagators of these excitations. In order to describe this aspect within a phenomenological approach, the constitutive equations of the present paper have to be generalised and supplemented by an equation of motion for the energy conservation, while the detection mechanism, equation (12), will remain unchanged.

This paper has benefited from many discussions of one of us (R.M.P) with H.Z. Cummins on the light scattering mechanisms. The latter was also instrumental in suggesting the collaboration that lead to the present paper.

References

1. L. Brillouin, Ann. Physique (Paris) **17**, 88 (1922)
2. E. Gross, Nature **126**, 201 (1930); *ibid.* **129**, 722 (1932)
3. L.D. Landau, G. Placzek, Physikalische Zeitschrift der Sowjetunion, **5**, 172 (1934)
4. R.D. Mountain, Rev. Mod. Phys. **38**, 205 (1966)
5. R.L. Murphy, J.T. Fourkas, W.X. Li, T. Keyes, Phys. Rev. Lett. **83**, 3550 (1999)
6. V.S. Starunov, E.V. Tiganov, I.L. Fabelinskii, JETP Lett. **5**, 260 (1967); C.I.A. Stegeman, B.P. Stoicheff, Phys. Rev. Lett. **21**, 202 (1968)
7. P. Bezot, G.M. Searby, P. Sixou, J. Chem. Phys. **62**, 3813 (1975); G.D. Enright, B.P. Stoicheff, J. Chem. Phys. **64**, 3658 (1976)
8. T. Keyes, D. Kivelson, J. Chem. Phys. **54**, 1786 (1971); H.C. Andersen, R. Pecora, J. Chem. Phys. **54**, 2584 (1971); *ibid.*, **55**, 1496 (1972)
9. M. Fuchs, A. Latz, J. Chem. Phys. **95**, 7074 (1991)
10. H.Z. Cummins, G. Li, W. Du, R.M. Pick, C. Dreyfus, Phys. Rev. E **53**, 896 (1996), *ibid.* E **55**, 1232 (1997)
11. C. Dreyfus, A. Aouadi, R.M. Pick, T. Berger, A. Patkowski, W. Steffen, Europhys. Lett. **42**, 55 (1998)
12. C. Dreyfus, A. Aouadi, R.M. Pick, T. Berger, A. Patkowski, W. Steffen, Eur. Phys. J. B **9**, 401 (1999)
13. A. Latz, M. Letz, Eur. Phys. J. B **19**, 323 (2001)
14. R. Schilling, T. Scheidsteger, Phys. Rev. E **56**, 2932 (1997)
15. T. Franosch, M. Fuchs, A. Latz, Phys. Rev. E **63**, 061209 (2001)
16. B.J. Berne, R. Pecora, *Dynamic Light Scattering*, (Dover Publications, Mineola, New York, 2000)
17. C. Dreyfus, M.J. Lebon, H.Z. Cummins, J. Toulouse, B. Bonello, R.M. Pick, Phys. Rev. Lett. **69**, 3666 (1992)
18. W.M. Du, G. Li, H.Z. Cummins, M. Fuchs, J. Toulouse, L.A. Knaus, Phys. Rev. E **49**, 2192 (1994)
19. A. Aouadi, C. Dreyfus, M. Massot, R.M. Pick, T. Berger, A. Patkowski, W. Steffen, C. Alba-Simionesco, J. Chem Phys. **112**, 9860 (2000)
20. G.Q. Shen, J. Toulouse, S. Beaufils, B. Bonello, Y.-H. Hwang, P. Finkel, J. Hernandez, M. Bertault, M. Maglione, C. Ecolivet, H. Z. Cummins, Phys. Rev. E **62**, 783 (2000)
21. G. Monaco, D. Fioretto, L. Comez, G. Ruocco, Phys. Rev. E **63**, 061502 (2001)
22. A. Tashin, R. Torre, M. Ricci, M. Sampoli, C. Dreyfus, R.M. Pick, Europhys. Lett. **56**, 407 (2001)
23. C. Glorieux, K.A. Nelson, G. Hinze, M.D. Fayer, J. Chem. Phys. **116**, 3384 (2002)
24. T. Franosch, A. Latz, R.M. Pick, Eur. Phys. J. B **31**, 229 (2003)